The role of glial peroxisome in neuron-glia communication in *Drosophila*

by

Maggie Sodders

A thesis submitted to the graduate faculty

in partial fulfillment of the requirements for the degree of

MASTER OF SCIENCE

Major: Genetics and Genomics

Program of Study Committee:
Hua Bai, Major Professor
Elizabeth McNeill
Clark Coffman

The student author, whose presentation of the scholarship herein was approved by the program of study committee, is solely responsible for the content of this thesis. The Graduate College will ensure this thesis is globally accessible and will not permit alterations after a degree is conferred.

Iowa State University

Ames, Iowa

2022

DEDICATION

This thesis is dedicated to my support system: Mom, Dad, Adam, Mady, and Scout.

TABLE OF CONTENTS

NOMENCLATURE

NMJ	Neuromuscular Junction
JAK-STAT	Janus kinases signal transducer and activator of transcription
ROS	Reactive Oxygen Species
upd3	Unpaired 3: *Drosophila* Protein
Pex5	Peroxin 5: *Drosophila* protein
NGS	Natural Goat Serum
Dome	Domeless: *Drosophila* Protein
Hop	Hopscotch: *Drosophila* Protein
JAK	Tyrosine Kinase in Mammals
STAT	Transcription Factor in Mammals

ACKNOWLEDGEMENTS

I would like to thank my committee chair, Hua Bai, and my committee members, Elizabeth McNeill, and Clark Coffman for their guidance and support throughout the course of this research.

In addition, I would also like to thank my friends, colleagues, the department faculty, and staff for making my time at Iowa State University a wonderful experience.

ABSTRACT

Peroxisome function in glial cells has been shown to impact neuronal functions. In the present study, we aim to elucidate the mechanism behind peroxisome-mediated glia-neuron communication using *Drosophila* as a model organism. I used the UAS-gal4 system to drive RNAi knockdown or overexpression in either glia tissue or motor neurons. The morphology of the axons directly preceding the abdominal neuromuscular junction (NMJ) was visualized using confocal microscopy and the axonal area and volume was quantified via ImageJ. Glial-specific knockdown of peroxisome import protein, Pex5, using pan-glial driver repo-gal4 resulted in increased axonal area and volume as compared to the control. Consistent with our previous work showing defective peroxisomes upregulate inflammatory cytokine upd3 and JAK-STAT signaling, overexpression of upd3 in glia increases axonal volume and area. We further show that neuronal-specific activation of the JAK-STAT pathway through hop overexpression results in an increase in axon size. Taken together, our findings suggest that impairment of peroxisomes in the glia impacts axonal morphology and potentially function via inflammatory response, specifically the JAK-STAT pathway.

THE ROLE OF GLIAL PEROXISOME IN NEURON-GLIA COMMUNICATION IN *DROSOPHILA*

Maggie Sodders, Hua Bai

Department of Genetics, Development, and Cell Biology, Iowa State University

Modified from manuscript to be Submitted to *G3: Genes, Genomes, Genetics*

Introduction

PEX genes make up an important gene family that produces peroxin proteins involved in the biogenesis of peroxisome organelles (Baumgart et al., 2001). In humans, mutations of PEX family genes cause disrupted peroxisome activity leading to peroxisome biogenesis disorders, including Zellweger's Syndrome. Important functional duties of the peroxisome are affected by these types of mutations include ether phospholipid (plasmalogen) biosynthesis, fatty acid alpha and beta oxidation, glyoxylate detoxification, and reactive oxygen species (ROS) regulation. Peroxisomal biogenesis disorders cause a range of symptoms affecting several organ types and systems, prominently including the liver as well as the renal and nervous systems. Neuronal symptoms of these disorders can include neurodevelopmental delays, progressive white matter disease, seizures, and neuronal migration disorders (Wanders and Waterham, 2006). Unfortunately, children inflicted with peroxisomal biogenesis disorders die early in life, usually prior to one year old (Baumgart et al., 2001). Several members of the PEX family can cause peroxisomal biogenesis disorders in humans including PEX 1,2,3,5,6,10,12,13,14,16,19, and 26 (Wanders and Waterham, 2006). In this study, we largely focus on an ortholog to peroxisomal biogenesis factor 5 (PEX5*)* in *Drosophila*, Peroxin 5 (Pex5) *(*Alliance, FBgn0023516*)*. Pex5 knockdown provides functional peroxisomal knockdown, allowing investigation of the peroxisome's role in glia-neuron communication.

Previously, it has been shown that impairment of peroxisome function, via knockout of peroxin, Pex5, in oligodendrocytes of mice causes a range of neuronal and neuromuscular phenotypes. Importantly, neuroinflammation, motor function decline, and cytokine levels increase in these animals as compared to controls. Phenotypes worsen significantly with age in adults, indicating continual defects as a result of peroxisomal import impairment. Glial tissue, however, seems largely unaffected by the knockout of Pex5 within oligodendrocytes themselves, including no differential cell survival in glial cells with and without this knockout. Eventually, mice with peroxisome deficient oligodendrocytes suffered axonal loss and death. One conclusion drawn from this study was peroxisomes in some glial subtypes provided axons with protection against neuroinflammation (Kassmann et al, 2007). In the present study, we aim to recapitulate some of these neuronal and neuromuscular phenotypes in *Drosophila* and identify mechanisms for how glial peroxisomes' function facilitates neuroprotection.

While the *Drosophila* nervous system is a well-established model for several neuronal diseases and studies, it does contain some inherent differences from the mammalian nervous system (Lu and Vogel, 2009; Jeibmann and Paulus, 2009). In this study, the focus is on the glia and neuronal cells of the peripheral nervous system of the *Drosophila*. The axon primarily used for analysis is about one node upstream from the neuromuscular junction with the A3 muscle of the *Drosophila* abdomen and is part of the ventral peripheral nervous system. In this area, on average each abdominal muscle receives ten axonal branches. (Hebbar et al., 2005). Glial cell types in the vicinity of the axon of interest for this study include wrapping glia, subperineural glia, and perineural glia. Generally, adult peripheral nervous system axons are individually encased by wrapping glia (Hartenstein, 2011). Wrapping glia have been phenotypically linked to Schwann Cells of the mammalian system (Stork et al., 2008). Outside the axons and wrapping glia lies a layer of subperineural glia,

which are known to create a blood-brain barrier via septate junctions. Finally, a layer of perineurial glia exists outside the subperineurial glia layer (Hartenstein, 2011). Axons directly proceeding the neuromuscular junctions are known to have subperitoneal glia lining the axons through the NMJ but wrapping glia ensheathment stops just above the muscle innervation (Freeman, 2015).

Following recapitulation in *Drosophila* of the initial peroxisomal stress phenotypes previously identified in mice, we identify the JAK-STAT pathway as a potential cause of increased neuroinflammation, enlargement in axons. Previously, our lab has shown knockdown of the cargo receptor Pex5 can induce peroxisomal import stress leading to an induction of unpaired 3 (upd3) in *Drosophila* oenocytes (hepatocyte-like cells). This induction was shown to be achieved via the c-Jun-N-terminal kinase signaling pathway in the tissue. In addition, overexpression of *Pex5* was able to block endogenous induction of upd3 in the oenocytes (Huang et al., 2020). We identify a similar pathway in the *Drosophila* glial cells causing an increase of these upd3 cytokines downstream of a Pex5 knockdown. Increased upd3 expression was also linked to increased activity in the Janus kinases signal transducer and activator of transcription (JAK-STAT) pathway. Specifically, in the oenocyte tissue, Pex5 knockdown was linked to a downstream increase in oxidative stress in the heart. Together, these data indicate an interorgan communication between the oenocyte and the heart mediated by peroxisomal stress and downstream JAK-STAT pathway activation (Huang et al., 2020). We aimed to identify similar communication occurring between glial and neuronal tissue that could be causing an increased inflammatory response in axonal tissue, leading to a swelling or enlargement phenotype in the axon.

Material and Methods

Fly Husbandry and Stocks

Flies were maintained at 25°C, 40% relative humidity and 12-hour light/dark. Adults were reared on agar-based diet with 0.8% cornmeal, 10% sugar, and 2.5% yeast (unless otherwise noted). Fly stocks used in the present study are: Mz97-gal4, Moody-gal4 (gifts from McNeill Lab), repo-gal4/Twist-GFP;Ser (a gift from McNeill Lab), w; P{UAS-upd3-GFP}attp40; + (a gift from Doug Harrison), UAS-hop[tuml];+;+ (a gift from Bach Lab), w;ok6-gal4;+ (BL64199), yw^R, Pex5i/CyO (BL58064) , TriPattp40 (BL36304), Repo-GS-gal4, and w^{1118} (BL5905) (Bloomington Stock Center). yw^R, w^{1118}, and TriPattp40 flies were used as controls in most of the experiments as specified. Only adult female flies were used in all experiments. For most experiments, adults raised to 7 days post eclosion, unless indicated otherwise. RU486 (mifepristone, Sigma, St. Louis, MO, USA) were used to activate Repo-GS-Gal4 at a final concentration of 200 μM mixed into the flies' food, similar amounts of ddH_20 were used in control flies' food.

Adult Abdominal Dissection

Adult *Drosophila* are anesthetized using flynap (Carolina, Burlington, NC) and placed in a dish with a light layer of Vaseline coating the bottom. Wings can be pushed into the Vaseline to secure the dish. Using scissors, a cut is made between the thorax and the abdomen. With tweezers, the head, thorax, legs, etc. can be removed from the dish. A solution of cold Ca^{2+} Free Media [128 mM NaCl, 2 mM KCl, 4 mM MgCl2(H2O)6, 35.5 mM sucrose, 5 mM HEPES, 1 mM EGTA, H2O, pH 7.2] is poured into the dish so carcasses are submerged. Flipped carcasses abdomen can now be exposed with the dorsal side facing up and cut off the very bottom of the abdomen. Next, cut carcass open along the dorsal midline and push cuticle sides into Vaseline for stability. Remove internal organs from the

carcass. This should expose fat bodies as well as underlying muscles. Using tweezers or the liposuction needle, carefully remove fat bodies from the central part of the abdomen. Be sure to remove everything obstructing the view of the midline muscles [protocol adapted from Wagner et al., 2015 and previously performed in Birnbaum et al., 2021].

Immunohistochemistry

Fixation using 4% paraformaldehyde for 20 min at room temperature followed tissue dissection. Tissue was subsequently washed in 1X PBST (0.1% Triton X) and blocked with 5% NGS (normal goat serum) at room temperature for one hour. Incubation in primary antibodies occurred overnight at 4°C with primary antibodies in 5% NGS 1X PBST [1X phosphate buffer saline, 0.1% Triton X-100]. Primary antibodies used were as follows: anti-Acetylated Tubulin (Sigma Aldrich T7451), anti-repo (DSHB 8D12), anti-ATP5A1 (Fisher 439800), and anti-Fly PMP70 (a gift from Kyu-Sun Lee Lab). Tissues were then washed in 1XPBST. Tissues were then incubated for 1.5 h at room temperature in 1XPBST at a dilution of 1:200 with secondary antibodies and kept in the dark at room temperature. Secondary antibodies included: 488 donkey anti-mouse, 647 donkey anti-mouse, rabbit anti-HRP-594, 488 anti-guinea Pig (Jackson ImmunoResearch Laboratories Inc, West Grove PA). Samples were washed in 1XPBST and mounted in Prolong Diamond (Life technologies).

Imaging and Analysis

Images were captured using Olympus FV3000 laser scanning confocal (Olympus, Waltham, MA, USA). Using a 40x lens with 20x digital zoom took images of axon one node above the neuromuscular junction terminal. Analysis was performed on ImageJ/Fiji (Schindelin et al., 2012). Entire axon is contained in the Z-slices of the images taken. If Axon has more than 30 Z-slices or less than 10 Z-slices, then they were excluded from quantification. Change Image Type to 8-bit. Specify an ROI to be 5 microns wide and 10

microns in length so it captures the most axonal tissue possible. For area analysis, max project this image and use the polygon tool in ImageJ to trace outline of axon. Using the measure function on ImageJ and record. For volume analysis, threshold image stack using OTSU threshold. Using the plugin Voxel Counter (Rasband, 2002) and record thresholded volume.

Climbing (Geotaxis) Assay

Climbing ability was measured via a negative geotaxis assay performed by tapping flies to the bottom of an empty glass vial and counting flies that climbed between nine and six centimeters, between six and three centimeters, or below three centimeters within 10 seconds as determined by a video recording. Flies were scored at ten days old and twenty-seven days for each genotype.

Calculations were done to 'score' climbing ability. The number of flies were counted in each of the three sections ten seconds after being tapped down. The number of flies in the top-most portion was multiplied by ten, the number of flies in the middle portion was multiplied by three, and the number of flies in the bottom portion were counted and multiplied by one. These scores were done on each vial, with one genotype per vial and averaged over the number of flies in each vial. Scores were calculated after each of five tap downs per vial per time point.

Statistics

GraphPad Prism (GraphPad Software) was used for statistical analysis. To compare the mean value of treatment groups versus that of control, a one-way student t-test using Welch's correction for unequal standard deviation was used. For comparing groups larger than two to controls, a one-way ANOVA with multiple comparisons analysis using Tukey correction. Before analysis, outliers were identified using Robust regression and Outlier

removal (ROUT) method (Q = 1%). * = $p<0.05$, ** = $p<0.01$, ***= $p<0.001$, ****=$p<0.0001$.

Results

Knockdown of Peroxin 5 in Repo-Positive Glial Cells is Positively Correlated with Increased Axon Area and Volume in the Drosophila Abdominal Peripheral Axons

Using confocal microscopy and immunofluorescent labeling we aimed to see if axons of the peripheral nervous system exhibited different phenotypes in controls as compared to the previously described Pex5 glial knockdown. Peroxisomes, identified by antibodies against PMP70, were visually confirmed to be endogenously expressed in the glial and neuronal tissues, as identified by antibodies against repo and horse radish peroxidase respectively (Figure 1A). The same axon was used for all subsequent axonal analysis. This axon is an abdominal axon in the peripheral nervous system, and the area used in this study is just above the last node of the axon prior to the neuromuscular junction with the A3 abdominal muscle (Figure 1B and 1C).

By crossing *Drosophila* lines with a UAS promotor linked to RNAi inhibiting the Pex5 protein with a pan-glial repo-gal4 line, I created a fly line with a knockdown of the Pex5 protein function withing glial tissue. Previously, it has been shown that knockdown of the ortholog protein, PEX5, in mice oligodendrocytes caused swelling of nervous tissue followed by degeneration of the tissue (Kassmann et al., 2007). Recapitulation of this phenotype in *Drosophila* with knockdown of the similar protein, Pex5, is crucial to determining the mechanism of the creation of this phenotype. As expected, seven-day old adult *Drosophila* with impaired peroxisomal function in glial cells showed an obvious change in axon size in the peripheral nervous system as compared to controls (Figure 2A). This change was confirmed with measurements of the axonal area and volume of a five by ten-micron immunolabeled image of these axons. Axon areas of these peroxisomal impaired flies

were significantly larger than either of the two control lines (Figure 2B). Additionally, measurements of axonal volume in these knockdown flies were significantly larger than a repo-driven transposon insertion control and a repo-driven yw control (Figure 2C). This is consistent with our expectations based on the observations made in studies of mice PEX5 knockouts in glial cells (Kassmann et al., 2007). These data indicate the enlarged axonal phenotype seen in mice with peroxin 5 disfunction in their oligodendrocytes can we phenocopied in the *Drosophila* peripheral nervous system.

To further confirm this phenotype, a geotaxis assay was performed to determine if, like the peroxisome oligodendrocyte knockout mice, the knockdown flies have impaired motor phenotypes (Kassmann et al., 2007) (Figure 2D). The assay was performed on flies of each genotype, two controls and the peroxisomal knockdown, at ten days old and twenty-seven days old. At ten days old, a comparable age to that which the axonal area and volume are determined, the peroxisomal knockdown flies were trending downward in climbing ability as compared to the control flies at the same time point (Figure 2E). However, at twenty-seven days old the Pex5 RNAi flies were significantly impaired in their climbing ability as compared to the two control lines (Figure 2D and 2E). Additionally, there was a near significant difference in climbing ability between the ten-day old knockdown flies and the twenty-seven-day old knockdown flies. These data indicate, as expected, the phenotypes associated with the partial knockdown of the Pex5 protein can be associated with motor defects and these phenotypes worsen with age in *Drosophila* as they do in the mouse model (Kassamann et al., 2007).

In order to confirm the knockdown this peroxin protein is acting in the adult stage, not just in developmental stages, we employed a gene-switch repo-gal4 driver. Using this driver, we knocked down the same Pex5 protein via RNAi at seven-days old and observed its axonal phenotype at fourteen-days old, or seven-days after the knockdown was activated via 200

mM RU feeding. Axonal area in these activated Pex5 knockdown animals was shown to be significantly higher than that of the control, inactivated animals (Figure 3A). The volume of the axon in these adult knockdown flies was significantly different than control (Figure 3B). Visually, the axons of the Pex5 knockdown flies appear to be larger than the control axons (Figure 3C). These data along with the results of the geotaxis assay indicate peroxisomal dysfunction as caused by Pex5 RNAi knockdown affect the adult peripheral nervous system.

RNAi Knockdown of Peroxisomal Import Protein 5 in Specific Subtypes of Glial in Drosophila can also induce an enlarged axon phenotype.

To further narrow down the glial cells responsible for the axonal enlargement phenotype, we performed a similar cross to that described previously, but with more specific glial cell drivers. The axon in the area we are analyzing have three glial subtypes surrounding it. The wrapping glia are immediately outside the axon, and the sub peritoneal glia are outside the wrapping glia. Lastly, surrounding both the wrapping and sub peritoneal glia, is the peritoneal glia (Hartenstein, 2011). Therefore, similarly knocked down Pex5 proteins using the Moody-gal4 driver, which has been shown to drive in sub perineural and perineural glia of the *Drosophila* peripheral nervous system as well as the Mz97-gal4 driver which largely drives in the wrapping glia but can also express in some sub perineural glia were used to identify the glial subtypes most responsible for the axonal enlargement phenotype (Yeh et al., 2018)**.** When paired with UAS linked Pex5 RNAi, both glial drivers visually phenocopied axonal enlargement seen in the pan-glial knockdown of the Pex5 protein (Figure 4A and 4B). When quantified, axonal area in Mz97-gal4 driven Pex5 knockdowns were significantly different from a control. Axonal area in Moody-gal4 driven Pex5 knockdowns were also significantly different from controls (Figure 4C). Axonal volume in both the Mz97 and Moody driven knockdowns of Pex5 protein were significantly different from their respective

controls (Figure 4D). These data indicate Pex5 function in multiple glial subtypes can contribute to axonal enlargement phenotype.

Impairment of Several Important Functions of the Peroxisome Can Contribute to the Axonal Phenotypes Seen in Knockdown of Peroxisomal Proteins in Repo-Positive Glial Cells

Impairment of the peroxin 5 impairs several critical functions performed by the peroxisome, and in many ways causes peroxisome biogenesis disorder phenotypes seen in human patients. Importantly, biogenesis of the peroxisome organelle requires Pex5 function (Cara et al., 2019). We aimed to narrow down which of these critical functions was the upstream cause of the axonal enlargement phenotype seen in the Pex5 knockdown. In order to achieve this, we used the same pan-glial driver, repo, used to knockdown Pex5 to knockdown three other peroxisomal proteins. ACOX1 is predicted to be involved in the synthesis of very-long-chain fatty acids (VLCFA) as well as production of ROS (Chung et al., 2020). GnPat, an ortholog of the human GNPAT protein, is predicted to be involved with the ether biosynthesis pathway in the peroxisome (Faust et al., 2012). The last protein, Catalase (Cat), is known to be involved in the mediation of reactive oxygen species (ROS) as facilitated by the healthy peroxisome (Mackay et al., 1989).

Visually, repo-driven RNAi knockdown of Acox1, GnPat, and Catalase proteins show similar axonal increases (Figure 5A). Notably, the Acox1 RNAi knockdown appeared to have the largest visual increase in axon size (Figure 5A). As expected, based on these visual representations, the Acox1 glial knockdown was found to have a significant increase in axonal area as compared to controls (Figure 5B). Acox1 knockdowns also show a significant difference from controls in axonal volume (Figure 5C). The GnPat glial knockdown showed a near significant increase in its axonal area when compared to two controls (Figure 5B). GnPat glial knockdown axonal volumes were significantly different from one of two controls (Figure 5C). The catalase glial knockdowns axonal area was not significantly different from

controls (Figure 5B). Similarly, axonal volumes of catalase glial knockdowns were not significantly different from both controls (Figure 5C). All two of the three peroxisomal proteins knockdowns showed phenotypes consistent with the knockdown of the original Pex5 glial knockdown (Figure 5A, 5B, and 5C). These data indicate several peroxisomal proteins and the lipid metabolism within glia could be contributing to axonal phenotypes.

The JAK-STAT Pathway in the Drosophila abdominal Peripheral Axons Cause a Similar Phenotype to the Knockdown of Peroxisomal Import Protein 5 in Repo-Positive Glial Cells and Are Hypothesized to be Downstream of the Peroxisome Impairment

Our lab has previously reported a link between the peroxin 5 and an increase of upd3 in the *Drosophila* oenocyte (Huang et al., 2020). Upd3 is a known activator of the JAK-STAT pathway in *Drosophila* (Copf et al., 2011). We hypothesize a similar process taking place in the *Drosophila* peripheral glial tissue could lead to an increase of JAK-STAT signaling in the nearby axon. If the Pex5 knockdown causes an increase in upd3 in the glial cells surrounding axons and signaling these axons to upregulate JAK-STAT machinery, then the overexpression of upd3 in glial tissue should cause the same cascade and eventual enlargement phenotype.

To test this, we overexpressed upd3 in glial tissue using the UAS-gal4 system and a pan-glial driver, repo. Visually, the glial upd3 overexpression axons phenocopied the Pex5 knockdown axons (Figure 6A). As expected, a statistically significant increase to axonal area was observed in these glial upd3 overexpression animals, when compared to controls (Figure 6C). Also as expected, axonal volumes in these animals were significantly different from controls (Figure 6D). These data indicate glial upd3 could be downstream of the glial Pex5 knockdown in the mechanism leading to axonal enlargement.

Using similar logic as outline above, we hypothesize upd3 can activate JAK-STAT receptors in the nervous system (Copf et al., 2011). In order to test this, we overexpressed

hop, a component of the JAK-STAT receptor machinery, in the motor neurons to see if a similar phenotype could be observed to that of the Pex5 knockdown and upd3 overexpression (Copf et al., 2011). Once again, a phenocopy of the axonal enlargement phenotypes previously observed could indicate a common pathway between Pex5 knockdown, upd3 overexpression, and hop overexpression.

OK6-gal4 was used to drive the overexpression of hop protein in the motor neurons. The phenotype was again visually recapitulated in these overexpression experiments (Figure 6B). As expected, a significant difference was observed between the axonal area of ok6 driven Hop expression animals and ok6 driven controls (Figure 6E). A significant increase in the axonal volume was also present in the hop overexpression animals as compared to a control (Figure 6F). These data could indicate a mechanism of axonal enlargement involving the JAK-STAT pathway.

Acetylated- Tubulin is Elevated in the Knockdown of Peroxisomal Import Protein 5 in Repo-Positive Glial Cells

After the nearby axon receives a signal from the peroxisomal impaired glia, a specific mechanism must take place to cause the axonal enlargement phenotypes observed. In order to elucidate the mechanism within the axon upstream of enlargement, we used an antibody against acetylated tubulin to visualize changes in membrane machinery of said axon. This antibody marking was performed on the genotypes identified to show this enlargement, Mz97-gal4 driven RNAi Peroxin 5 knockdown, as well as a control. Quantification of AcTub was performed similarly to quantification of HRP labeled axons in this study. Using HRP antibodies to identify the axonal area previously quantified, the same area was evaluated for differential acetylated tubulin phenotypes.

The amount of acetylated tubulin visually appears to be much larger in glial Pex5 knockdown animals than in controls (Figure 7A). Indeed, area and volume calculations of

both the knockdown and control areas were significantly different from one another (Figure 7B and 7C). This phenotype requires further evaluation to be definitive but can be used a starting point for further analysis of inner axonal mechanisms for the axonal enlargement phenotype.

Discussion

First, establishment of the presence of peroxisomes in and around the glial tissue at the axon of interest for this study was accomplished. Since peroxisomes exist in this area, we expect a knockdown of their function to cause local effects on the animal. In addition, I identified a consistent area directly above neuromuscular junction (NMJ) at the A3 muscle can be used as a model for the peripheral nervous system in *Drosophila.*

Kassmann et al. in 2007 identified swelling of axonal tissue, preceding axonal degeneration, in mice with a PEX5 knockout in oligodendrocytes. We were able to phenocopy this result in *Drosophila* with a Pex5 knockdown, via RNAi, in most glial tissue. Specifically, axons within animals having a pan glial Pex5 knockdown are significantly larger in area, and in volume. Theses phenotypes are indicative of potential axon swelling but confirms axonal enlargement as a result of the peroxisomal protein knockdown.

In addition to axonal enlargement phenotypes, mice with impaired oligodendrocyte peroxisome function exhibited motor ability declines that worsened with age (Kassmann et al., 2011) In order to assess the motor abilities of our pan glial Pex5 knockdown flies, a climbing assay was performed. This assay gave us several important insights. At ten days old, an age comparable to the seven-days old that is used for other assays, slight decrease in motor ability is seen. This indicates that around the same time axons have been shown to have an enlargement phenotype, there is some motor ability decline. Later, at twenty-seven days old, a significant decrease in motor ability is seen as compared to twenty-seven-day old controls. This result indicates the knockdown of Pex5 in glia cells affects not only axon size, but also

flies' motor abilities. In addition, a near significant difference is observed between the motor abilities ten-day old Pex5 knockdown flies and twenty-seven-day old knockdown flies. The decline in motor function with age is similar to the mice phenotype decline seen in Kassmann et al. 2007 paper and indicates a worsening of symptoms with age. Further these results suggest peroxisome dysfunction is causing adult specific phenotypes.

In order to assess if adulthood is a critical stage for these axonal phenotypes, we employed the use of a repo-geneswitch-gal4. The gene-switch, and subsequent activation of Pex5 RNAi, was turned on seven days old, after the adult abdominal NMJ is fully remodeled (Hebbar et al., 2005). After seven days of Pex5 knockdown activation, so at fourteen days old, the flies were dissected and subject to similar techniques as performed on the non-gene-switch animals. Axonal area and volumes were similar to the constitutive repo-gal4 knockdown results. Specifically, a significant difference in axon area was observed and a significant difference in axon volume was also observed. These results indicate the adult stage axons are being affected by glial Pex5 knockdown. It is important to note, no other time points were assayed, so we cannot rule out this knockdown having more or less effects at different developmental stages. However, these results in combination with the differential motor phenotypes seen between ten- and twenty-seven-day old Pex5 knockdowns together indicate the adult stage as an important period for axonal enlargement phenotypes.

In addition to the pan-glial, repo-driver, we wanted to investigate how driving the Pex5 knockdown in specific subtypes of glia affect the axonal phenotypes. To this end, I first drove the same Pex5 RNAi knockdown in Mz97-gal4, which is a driver primarily active in wrapping and subperineural glia. These two subtypes of glia are the ones directly surrounding the axon of interest in the present study (Freeman, 2015). Mz97-driven knockdown of Pex5 shows similar axonal area, with significant increase from control, and axonal volume, with significant increase from control, as the pan-glial Pex5 knockdown. In fact, the axonal

volume phenotype is potentially stronger in the Mz97 driven knockdown than the repo driven knockdown. This response could have several possible reasons including because Mz97 is more centered on glial tissue directly surrounding affected axon, but also the driver strength could potentially play a role. Overall, these data indicate driving the peroxin 5 knockdown in wrapping and subperineural glia can elicit a similar, if not stronger, response in the axon as driving the same knockdown in pan-glial repo.

In addition to the Mz97-gal4 driver, we employed the Moody-gal4 driver. Moody is a driver primarily active in sub perineural glia but may also express in some other glia subtypes such as wrapping and perineural glia (Yeh et al., 2018)**.** Similar to the pan-glial knockdown of Pex5, Moody-specific knockdown of Pex5 shows a significant difference in axon area as well as a significant increase in axon volume when compared to controls. The Moody Pex5 knockdown does not seem to elicit as strong a response in axon volume as the Mz97 knockdowns. However, it should be noted, these data in particular have a low n that could affect significance testing, and driver strength could play a role. Nevertheless, a similar increase in axon volume and area indicates the subtypes of glia driven in moody do affect the axon enlargement phenotype. Taken together, the knockdown of Pex5 in the Mz97- and Moody-gal4 drivers indicates several subtypes of glia can play a role in the downstream axonal phenotypes.

In addition to testing the effect of different subtypes of glia on the Pex5 knockdown's eventual axonal enlargement phenotype, we wanted to see if impairment of a particular function of the peroxisome was primarily responsible for the downstream phenotypes seen in the glial Pex5 knockdowns. Pex5 functions as a cargo importer for the peroxisome, so knockdown of this protein affects several, if not all, function of the peroxisome. To this end, RNAi knockdowns were driven in the pan-glial driver for three peroxisomal proteins. First, Acox1 was knocked down. Acox1 is predicted to be involved in the very- long- chain fatty

acid (VLCFA) Beta-oxidation pathway in peroxisomes. This pathway eventually leads to H_2O_2 regulation, and therefore knockdown of this protein is hypothesized to impair this function of the peroxisome. Acox1 has also been associated with axonal loss, both via loss of function and gain of function mutations (Chung et al., 2020). Second, GnPat was knocked down. The GnPat protein is predicted to play a role in ether biosynthesis and could also cause impairment of the ether biosynthesis pathway (Faust et al., 2012). Lastly, Catalase was knocked down. Catalase is a protein known to be involved the ROS metabolism function performed by healthy peroxisomes (Mackay et al., 1989). The knockdown of the catalase protein could inhibit this ROS metabolism in the peroxisomes. Any one of these proteins phenocopying the axonal enlargement phenotypes seen when Pex5 is knocked down in glial cells could be informative for which function(s) of the peroxisome are important for downstream axonal enlargement and therefore, glial-neuronal communication and signaling.

Pan-glial knockdown of Acox1 and GnPat, but not Catalase peroxisomal proteins showed similar axonal enlargement phenotypes to pan-glial Pex5 knockdown. Both Acox and Gnpat glial knockdowns showed significant differences in axonal area as compared to controls. Catalase glial knockdown axons were not found to be significantly different than controls. Both Acox1 and GnPat glial knockdowns showed significant volume differences when compared with controls. Catalase glial knockdown axons, once again, were not found to be significantly difference from either control. Taken together these data indicate more than one peroxisomal protein dysfunction can cause an axonal enlargement phenotype, but not all peroxisomal functions and associated proteins are important for axonal size phenotypes. Specifically, these data indicate lipid regulation, via ether biosynthesis and very-long- chain fatty acid (VLCFA) Beta-oxidation, in glia is affecting axon size.

Thus far, we have established that peroxisomal stress, in the form of Pex5 and other peroxisomal protein knockdowns can cause the axon to enlarge when driven in glia cell.

Next, we try to determine mechanism after peroxisomal stress in glia and before axonal enlargement and motor phenotypes seen. Previous work in our lab showed a link between Pex5 knockdown and increase of the upd3 cytokine in *Drosophila* oenocytes (Huang et al., 2020). Based on this previous study, we hypothesized an upd3 increase in glia following peroxisomal stress in glia. To test this hypothesis, we overexpressed, using the gal4 UAS system, upd3 in pan-glial tissue to identify if a similar phenotype to the pan-glial knockout of Pex5 occurred. Indeed, this glial upd3 overexpression resulted in similar phenotypes as pan glial knockdown of Pex5. Specifically, a significant increase in axonal area axonal volume was observed in the glia driven upd3 overexpression axons. These data indicate Pex5 knockdown and upd3 overexpression are part of the same pathway leading to the axonal enlargement phenotype.

Previous studies have found a link between the upd3 cytokine and activation of the JAK-STAT pathways in *Drosophila,* including studies done in our lab in the oenocyte tissue (Huang et al., 2020). The JAK-STAT pathway in mammals has been linked to transcriptional activation of several immune-related genes, including being able to increase the expression of more than thirty cytokines (Agaisse and Perrimon, 2004). One of the phenotypes observed in mice with oligodendrocyte specific knockout of Pex5 was an eventual increase of cytokines in the brain (Kassmann et al., 2007). Therefore, investigation of the link between the Pex5 knockdown in *Drosophila* and the corresponding *Drosophila* upd3 induced JAK-STAT pathway could be a good candidate for elucidating the mechanism leading to the eventual phenotypes seen in both Pex5 KD *Drosophila* and Mice.

The JAK-STAT pathway in *Drosophila* contains four primary components. This pathway's components have been shown to be present in the *Drosophila* brain (Copf et al., 2011). The first component is the ligand, of which the three unpaired proteins are known to be (Agaissee and Perrimon, 2004). In this study, we identify upd3 to be the ligand of interest.

Upd3 is IL-6 – like ligand in the *Drosophila* system (Copf et al., 2011). The ligand interacts with the domeless (Dome) receptor in the extracellular space (Agaissee and Perrimon, 2004). Dome is an IL-6 receptor-like *Drosophila* protein (Copf et al., 2011). In the present study, the Dome proteins on the surface of the axon of interest are thought to be interacting in the extracellular space with the upd3 ligand secreted from nearby glial cells. In the cell, Dome has proteins it interacts with that act like the mammalian JAK and STAT proteins (Copf et al., 2011).

The *Drosophila* protein acting in a JAK manner is the Hop protein and the *Drosophila* protein acting in a STAT-like manner is the STAT92E protein (Agaisse and Perrimon, 2004). In previous studies, upd3 was shown to induce the phosphorylation and activation of the Hop protein, and Dome has been shown to signal through the Hop-STAT92E machinery (Agaisse and Perrimon, 2004). Based on this information and our upd3 overexpression results, we hypothesized upd3 increases in glial tissue could exit the glial cell and activate JAK-STAT machinery in the axons via the Dome receptor. The increase of the JAK-STAT pathway could then be acting to increase inflammation in the axon, resulting in the enlargement phenotype documented in the present study (Copf et al., 2011). This pathway could also potentially explain the neuroinflammation phenotype seen in the brains of Mice with Pex5 oligodendrocyte knockouts (Kassmann et al., 2007).

JAK-STAT signaling in Mammals, including humans, has been shown to be involved in the innate immune response, including neuroinflammatory responses. Indeed, abnormal JAK-STAT pathway activation has been linked too Multiple Sclerosis and Parkinson's disease, both of which are considered to be neuroinflammatory diseases. JAK-STAT activation has been shown to contribute to inflammation as a pathogen response (Yan et al., 2018). In *Drosophila*, JAK-STAT signaling pathway has been shown to increase immune-related genes and cause differential immune cell differentiation upon activation (Myllymäki

and Rämet, 2014). Therefore, further studies should be done to identify if the activation of the JAK-STAT pathway in the context of glial peroxisomal stress is causing an inflammatory response leading to the axonal enlargement phenotype observed in the present study and/or the neuroinflammation observed in mice with similar peroxisomal defects (Kassmann et al., 2007).

To test the activation of JAK-STAT in axons and see if activation produced a similar phenotype to glial Pex5 knockdown and upd3 overexpression, we overexpressed Hop, a protein component of the JAK-STAT machinery, in motor neurons. This Hop overexpression was also done via the UAS, gal4 system, but this time using OK6-gal4 as the driver. As part of the JAK-STAT machinery, if upd3 expression was activating JAK-STAT, Hop would be expected to also be activated and cause a similar downstream phenotype.

As expected, ok6 driven Hop overexpression did cause axonal area and axonal volume to increase significantly. In fact, hop overexpression showed a stronger phenotype in terms of statistical significances, versus controls, than previous Pex5 glial knockdown and upd3 glial overexpression. This could be a result of JAK-STAT machinery being closer in sequence to the eventual axonal enlargement phenotype than either of the glial knockdowns. In any case, these data indicates that axonal hop overexpression, and consequently JAK-STAT overexpression, is in the same pathway as glia Pex5 knockdown and upd3 overexpression. These data also indicate the JAK-STAT pathway increasing is a viable mechanism for this axonal enlargement phenotype.

Lastly, we began investigating methods for axonal increase after JAK-STAT activation. Specifically, we aimed to identify what components of the axon are becoming enlarged to cause the total axon enlargement phenotype. To this end, we investigated the amount of acylated-tubulin to see if there were changes total area and volume of this component in repo driven Pex5 knockdowns versus controls. Significant differences in

acylated tubulin area and volume were identified via measurement of Acylated tubulin immunostaining, with co-HRP immunostaining to identify acetylated tubulin in the axon of interest. This, however, not enough information to draw a link between this increase and overall axonal area increase. Consequently, further studies will be required to determine if acylated-tubulin contributes to axonal enlargement phenotype as well as any other contributors to this phenotype, including neuroinflammation.

Based on these results, a model of the pathway between peroxisomal stress and axonal enlargement in the *Drosophila* abdominal axons. Specifically, peroxisome stress leads to an increase in the cytokine upd3. Upd3 then activates the JAK-STAT pathway in the axon of interest, and JAK-STAT activation causing axonal enlargement. Other studies will be needed to confirm this pathway, but the data presented here provides ample evidence indicating the existence and order of the pathway.

The elucidation of this pathway could have potential benefits for understanding neuroinflammation diseases as well as peroxisomal biogenesis disorders in humans. As previously mentioned, dysfunction or mis regulation of JAK-STAT signaling has been connected to known neuroinflammatory diseases, such as Multiple Sclerosis (Yan et al., 2018). These results could be reason to investigate the role of glia and specifically glial peroxisomes in initiation of this diseases associated JAK-STAT mis regulation. This pathway could also indicate mechanisms contributing to the neuronal disease phenotypes present in patients with peroxisomal biogenesis disorders, and again point in the direction of glial peroxisomes as an instigator in the processes leading to these phenotypes.

Adult *Drosophila* peripheral nervous system in the abdominal area is not a well-defined or oft studied area of this model organism's anatomy. This study presents some phenotypes can be studied in this area of the *Drosophila* nervous system that indicate the usefulness of using this area for investigation in future studies.

Conclusion

Overall, these data indicate a pathway from peroxisomal stress in glia to axonal enlargement in the peripheral nervous system axons around the A3 abdominal muscle in *Drosophila.* Specifically, our data indicates peroxisomal stress, from a pan glial Pex5 knockdown throughout development or specifically in adults, can cause axonal area and volume to increase Pan-glial driven Pex5 knockdown can also cause *Drosophila* climbing ability to decline over time. The axonal area and volume phenotypes also occur when Pex5 is knocked down in specific glia subtypes, namely sub perineural and wrapping glia. Peroxisomal stress in glia caused by knockdown of other peroxisomal proteins, Acox1, GnPat, and Catalase, can also cause axonal enlargement phenotypes. These peroxisomal proteins contribute to various peroxisomal functions, so multiple types of function peroxisome impairment can cause downstream effects in the axon. Downstream of glial peroxisomal stress, we hypothesize a glial upd3 increase in expression, which we show results in a similar axonal area and volume phenotype as the Pex5 glial knockdown axons. Downstream of glial upd3 expression, we hypothesize an increase in axonal JAK-STAT machinery. This is supported by the axonal overexpression of JAK-STAT component hop resulting in strong axonal enlargement phenotypes (Figure 8). This pathway could serve as a model for further research on the neuronal phenotypes indicative of Zellweger's syndrome as well as peripheral nervous system diseases with a neuroinflammation component. Further, these studies indicate the adult *Drosophila* abdominal innervation to be a viable model for communication and interactions between glial and neuronal cells.

FIGURES

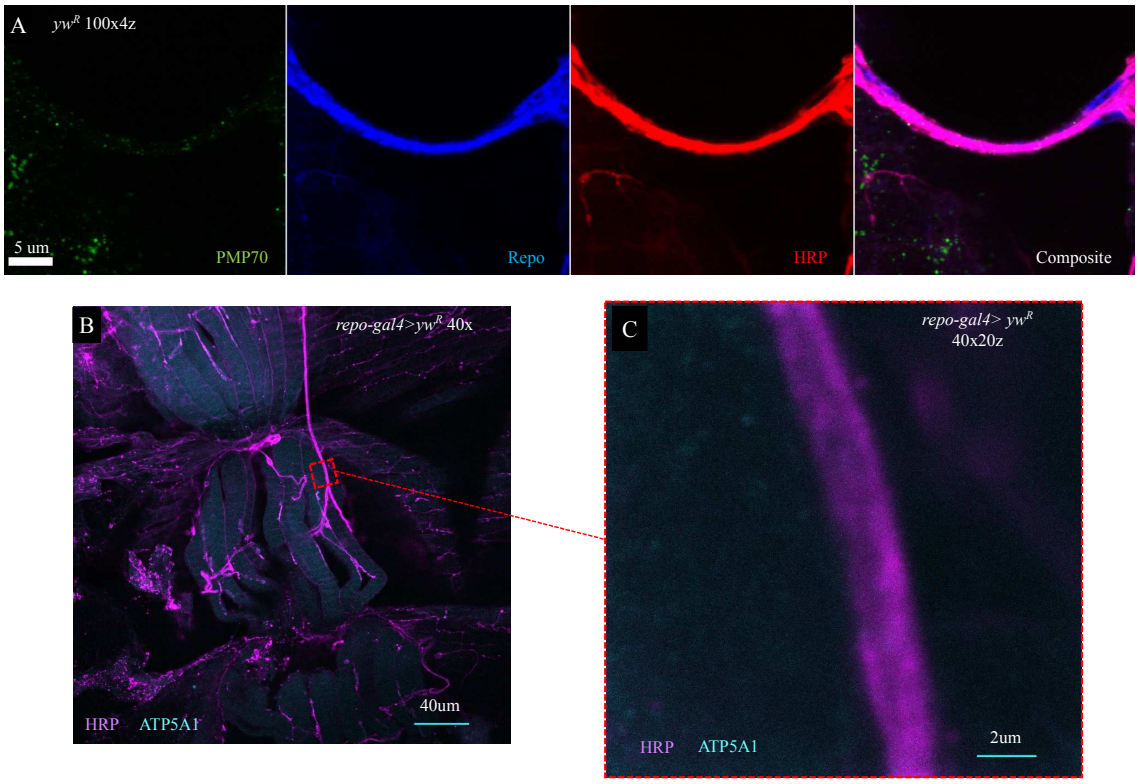

Figure 1: Peripheral Nervous System of *Drosophila* in close proximity to the Abdominal muscle, A3 in adults.

(A) A wild type, ywR, adult seven-day old fly various markers are shown identifying an axon slightly upstream of the peripheral axon used in subsequent analyses. From left to right, the axon is labeled with, (green) PMP70 peroxisomal marker, (blue) repo glial marker, (red) HRP neuronal marker, and a composite image of all markers merged. (B) Visual of the A3 abdominal muscle and associated peripheral nerves. HRP labeled neuronal tissue is indicated in magenta and ATP5A1 mitochondrial staining, cyan, allows for easy visualization of the A3 abdominal muscle in a control adult *Drosophila*. Red dashed box indicates area seen in (C) C a visual of the same axon seen in B with an additional digital zoom. This area, cropped to a five by ten micron is used for axonal area and volume quantifications.

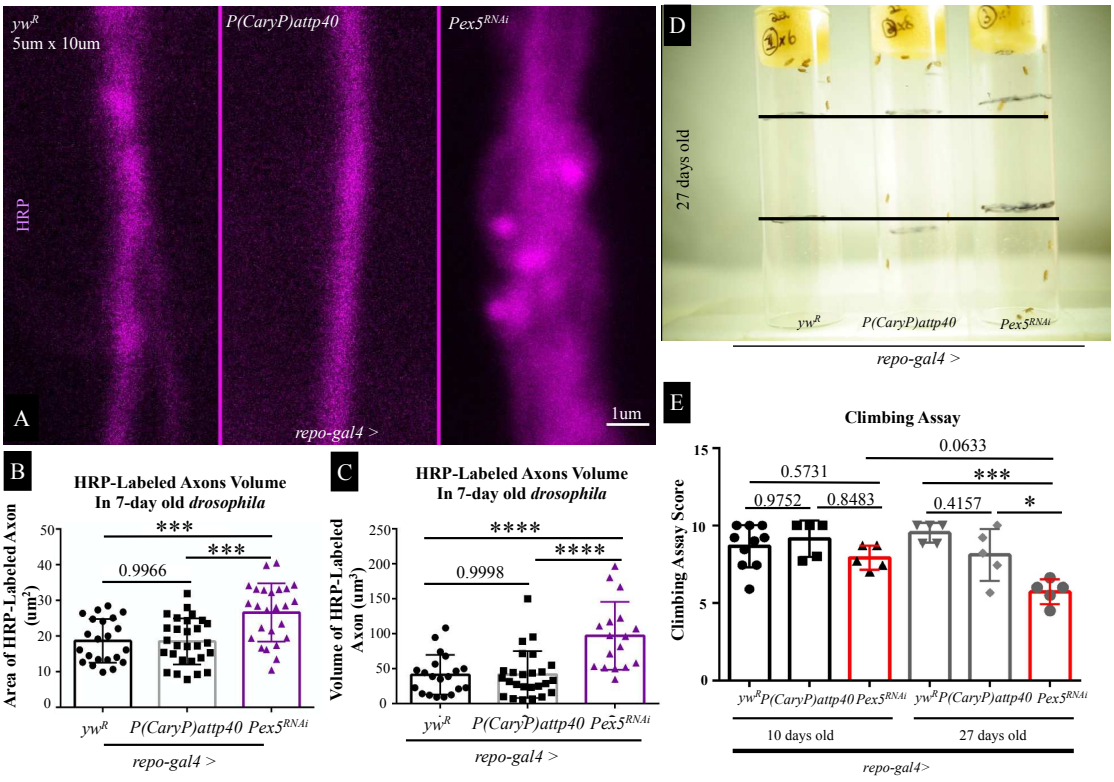

Figure 2: Knockdown of Peroxisome Import Protein 5 in the *Drosophila* glial cells initiates an axonal enlargement phenotype of the axons in the ventral peripheral nervous system.

(A) Axons of the ventral peripheral nervous system as identified by Horseradish Peroxidase antibody. Two control axons, *repo-gal4>yw*^{R} and *repo-gal4>P(CaryP)attp40* are show in the left and middle panels respectively. The *repo-gal4>Pex5*^{RNAi} Knockdown axon is show in the right panel. (B) Compiled and statistically evaluated two-dimensional area of axons in the *Drosophila* ventral abdominal nerves. The *repo-gal4>Pex5*^{RNAi} Knockdown flies has much larger axon size (purple) than either of the repo-gal4 driven controls. Statistical values are based on a data set cleared of outliers using a ROUT test being subjected to a one-way ANOVA with Tukey correction for multiple comparison. (C) Compiled and statistically evaluated volume, measured in voxels, of axons of the *Drosophila* ventral abdominal nerves. The *repo-gal4>Pex5*^{RNAi} Knockdown flies have a larger axon volume (purple) than either of

the repo-gal4 driven controls. Statistical values are based on a data set cleared of outliers using a ROUT test being subjected to a one-way ANOVA with Tukey's correction for multiple comparisons. (D) Set up of the geotaxis assay performed. 27-day old flies of each genotype are shown ten seconds after being tapped down for the first time. Black lines represent 6cm and 3cm from the bottom of the vial. (E) Geotaxis assay data and statistical representations. Left three samples based on each of the genotypes climbing assay scores at ten days of age. Black columns represent controls, and red column labels the *repo-gal4 > Pex5*^{RNAi} knockdown. No statistically significant differences seen between these knockdown flies and controls, but a trend downward in climbing assay score is seen at ten days old as compared to controls. Right three samples based on each of the genotypes climbing assay scores at twenty-seven days of age. Grey columns represent controls, and red column labels the *repo-gal4> Pex5*^{RNAi} knockdown. A significant difference exists between the Pex5 knockdown flies at ten and twenty-seven days old. Additionally, a difference is seen between the Pex5 knockdown and control flies at twenty-seven days of age. All statistics performed on data controlled for outliers via ROUT analysis then subjected to a one-way ANOVA with Tukey's correction for multiple comparison.

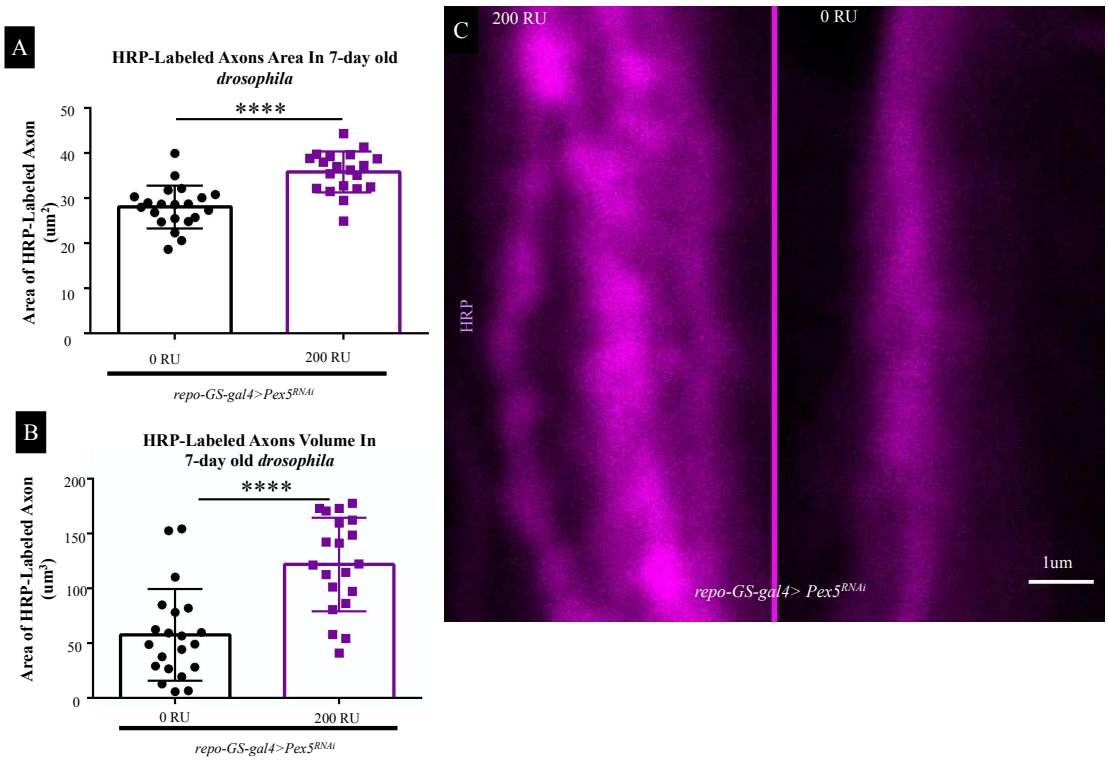

Figure 3: Knockdown of Peroxisome Import Protein 5 in the Adult *Drosophila* glial cells initiates an axonal enlargement phenotype of the axons in the ventral peripheral nervous system.

(A) Compiled and statistically evaluated two-dimensional area of axons in the *Drosophila* ventral abdominal nerves. The *repo-GS-gal4>Pex5^{RNAi}* RU fed knockdown flies has much larger axon size (purple) than the *repo-GS-gal4>Pex5^{RNAi}* driven controls. Statistical values are based on a data set cleared of outliers using a ROUT test being subjected to a one-way t-test with Welch's correction for unequal standard deviation. (B) Compiled and statistically evaluated volume of axons in the *Drosophila* ventral abdominal nerves. The *repo-GS-gal4>Pex5^{RNAi}* RU fed knockdown flies had a much slightly larger axon size (purple) than the *repo-GS-gal4>Pex5^{RNAi}* driven controls. Statistical values are based on a data set cleared of outliers using a ROUT test being subjected to a one-way t-test with Welch's correction for unequal standard deviation (C) Axons of the ventral peripheral nervous system as identified

by Horseradish Peroxidase antibody. Axons of *repo-GS-gal4> Pex5*^{RNAi} with RU feeding activating gene-switch activity and subsequent knockdown is shown in the left panel. Control axons, *repo-GS-gal4> Pex5*^{RNAi} without RU feeding activating gene-switch activity is shown in the right panel.

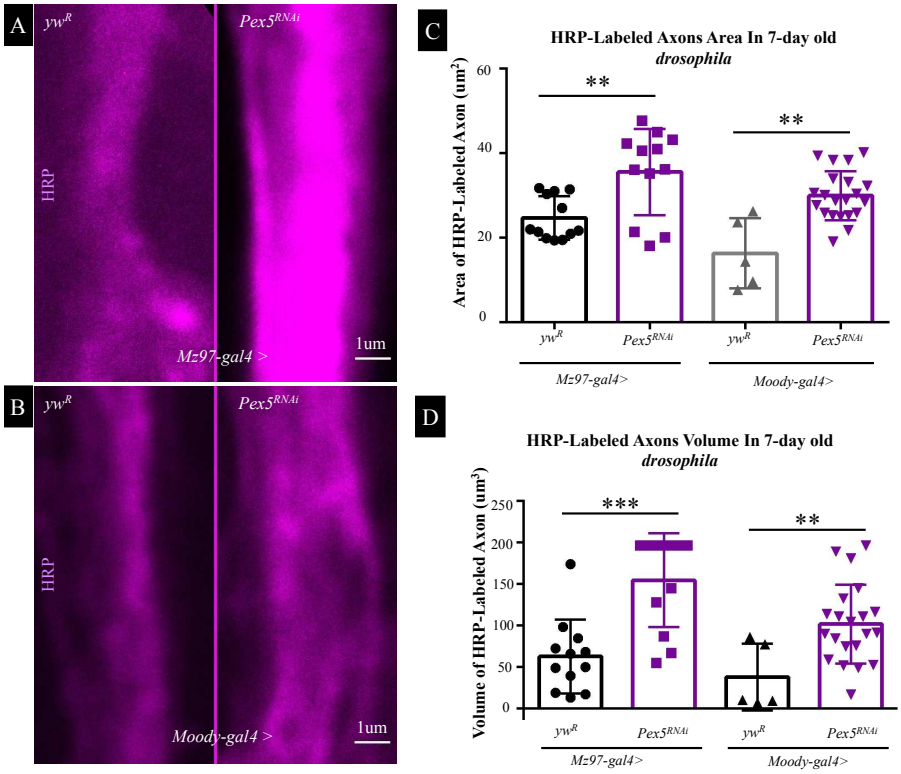

Figure 4: Peroxisome Import Protein 5 deficient in specific Glial subtypes driven by Mz97-gal4 and Moody-gal4 have similar downstream axonal phenotypes to the Pan-glial knockdown.

(A) Visual comparison between in a Mz97-gal4 driven control and Pex5^{RNAi} ventral peripheral axons. Neuronal tissue is labeled with Horseradish Peroxidase in magenta. (B) Visual comparison between Moody-gal4 driven control and Pex5^{RNAi} ventral peripheral axons. Neuronal tissue is labeled with Horseradish Peroxidase in magenta. (C) Compiled and statistically evaluated two-dimensional area of axons in the *Drosophila* ventral abdominal

nerves. Column in black indicates a *Mz97-gal4 > yw*^{R} control, and the grey column a *Moody-gal4> yw*^{R} control. The purple columns indicate Mz97-gal4 and Moody-gal4 drivers of Pex5^{RNAi}. Axonal area of Pex5 knockdowns driven by Mz97-gal4 is significantly different than its control. Axonal area of Pex5 knockdowns driven by Moody-gal4 is significantly different as compared to its control. Statistical values are based on a data set cleared of outliers using a ROUT test being subjected to a one-way t-test with Welch's correction for unequal standard deviation. (D) Compiled and statistically evaluated volume of axons in the *Drosophila* ventral abdominal nerves. Genotypes and color scheme indicated in graph are identical to those described in C. Axonal volume in Pex5 knockdowns driven by Mz97-gal4 are significantly different than controls. Axonal volumes in Pex5 knockdowns driven by Moody-gal4 are also significantly different than controls. Statistical values are based on a data set cleared of outliers using a ROUT test being subjected to a one-way t-test with Welch's correction for unequal standard deviation.

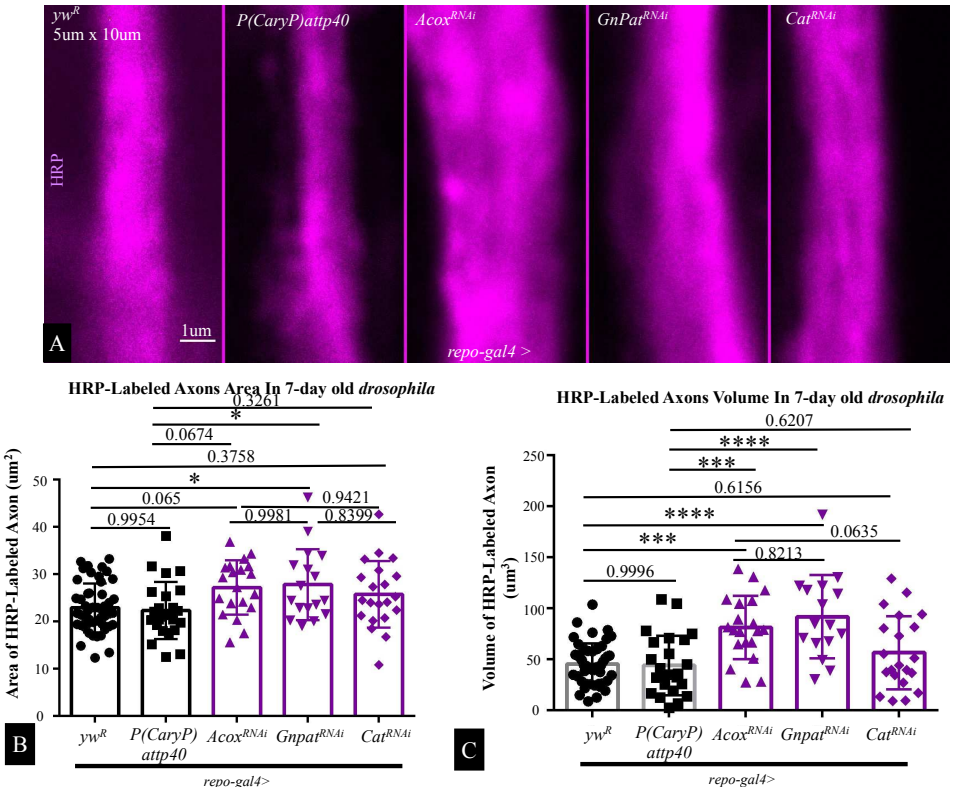

Figure 5: Knockdown of Other Peroxisomal Proteins driven in glial tissue elicit similar responses in the axon to knockdown of Pex5.

(A) Horseradish Peroxidase, magenta, labelled axons in different repo-gal4 driven RNAi knockdowns as well as two controls. From left to right, two controls are represented followed by Acox knockdown, GnPat knockdown, and Catalase (Cat) knockdown. (B) Compiled and statistically evaluated two-dimensional area of axons in the *Drosophila* ventral abdominal nerves. First two columns in black indicates a *repo-gal4> yw*^{R} control and *repo-gal4 >P(CaryP)attp40* control, which are statistically not different from one another. The following three purple columns indicate RNAi knockdowns of peroxisomal proteins Acox, GnPat, and Catalase, respectively. Axonal area of Acox knockdown is close to significantly different than both controls. Axonal area of GnPat knockdown is significantly different than both controls. Axonal area of Catalase knockdown is not significantly different than either control. Statistical values are based on a data set cleared of outliers using a ROUT test being

subjected to a one-way ANOVA with Tukey's correction for multiple comparison. (C) Compiled and statistically evaluated volume of axons in the *Drosophila* ventral abdominal nerves. Genotypes and color scheme indicated in graph are identical to those described in B. Axonal volume of Acox knockdown is significantly different than both controls. Axonal area of GnPat knockdown is significantly different than both controls. Axonal area of Catalase knockdown is not significantly different than either control. Statistical values are based on a data set cleared of outliers using a ROUT test being subjected to a one-way ANOVA with Tukey's correction for multiple comparison.

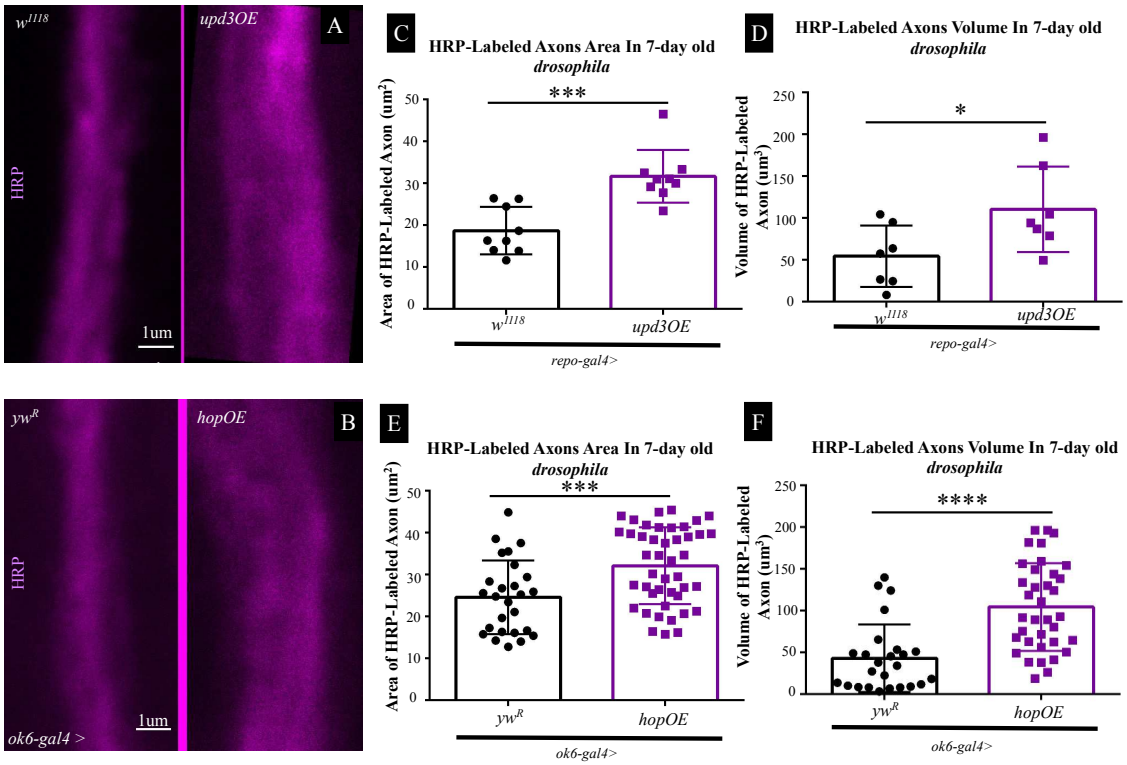

Figure 6: upd3 overexpression in driven in glial tissue results in a similar phenotype to knockdown of peroxisomal proteins in glia. Overexpression of JAK-STAT machinery component, hop, in motor neurons also results in axonal enlargement phenotypes.

(A) Visual representation of repo-gal4 driven w^{1118} controls (left) and repo-gal4 driven upd3 (right) axon size. Axonal tissue is labeled by antibody against horseradish peroxidase. (B) Visual representation of ok6-gal4 driven yw^{R} control (left) and ok6-gal4 driven hop (right) axon size. Axonal tissue labelled by antibody against HRP. (C) Graphical representation of axonal size in controls (black) and upd3 overexpression (purple) in glial tissue. upd3 overexpression axonal sizes were significantly different from controls. Statistical values are based on a data set cleared of outliers using a ROUT test being subjected to a one-way t-test with Welch's correction for unequal standard deviation. (D) Compiled and statistically evaluated volume of axons in the *Drosophila* ventral abdominal nerves. Genotypes and color scheme indicated in graph are identical to those described in B. upd3 overexpression axonal volumes were significantly different from controls. Statistical values are based on a data set cleared of outliers using a ROUT test being subjected to a one-way t-test with Welch's correction for unequal standard deviation. (E) Compiled and statistically evaluated two-dimensional area of axons in the *Drosophila* ventral abdominal nerves. Ok6-gal4 motor neuron driver was used to drive a yw^{R} control (black) and hop (purple) overexpression. Hop motor neuronal overexpression axon size is significantly different than controls. Statistical values are based on a data set cleared of outliers using a ROUT test being subjected to a one-way t-test with Welch's correction for unequal standard deviation. (F) Compiled and statistically evaluated volume of axons in the *Drosophila* ventral abdominal nerves. Genotypes and color scheme indicated in graph are identical to those described in E. Axonal volume in hop overexpression animals is significantly different than controls. Statistical values are based on a data set cleared of outliers using a ROUT test being subjected to a one-way t-test with Welch's correction for unequal standard deviation.

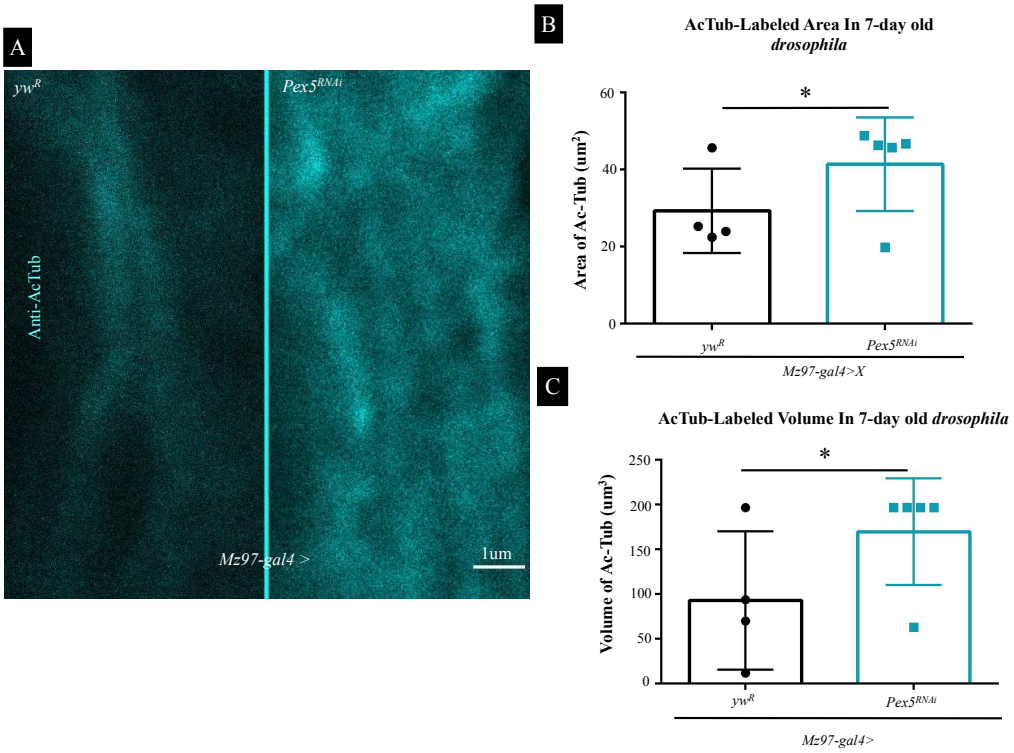

Figure 7: Acetylated Tubulin Expression in Mz97-gal4 driven Pex5 RNAi knockdowns

(A) Representative images in Mz97-gal4 driven control and Pex5 knockdown animals at the axon previously identified in this study. Antibody against AcTub in cyan is shown.

(B) Graphical representation of acetylated tubulin within an axon's size in controls (left) and $Pex5^{RNAi}$ knockdown (right) in Mz97-driven glial tissue. Control and knockdowns were significantly different. Statistical values are based on a data set cleared of outliers using a ROUT test being subjected to a one-way t-test with Welch's correction for unequal standard deviation. (C) Compiled and statistically evaluated volume, of acetylated tubulin in the *Drosophila* abdominal nerves. Genotypes and scheme indicated in graph are identical to those described in B. There was a statistical difference between control and Pex5 glial RNAi knockdown volumes, though n was quite low. Statistical values are based on a data set cleared of outliers using a ROUT test being subjected to a one-way t-test with Welch's correction for unequal standard deviation.

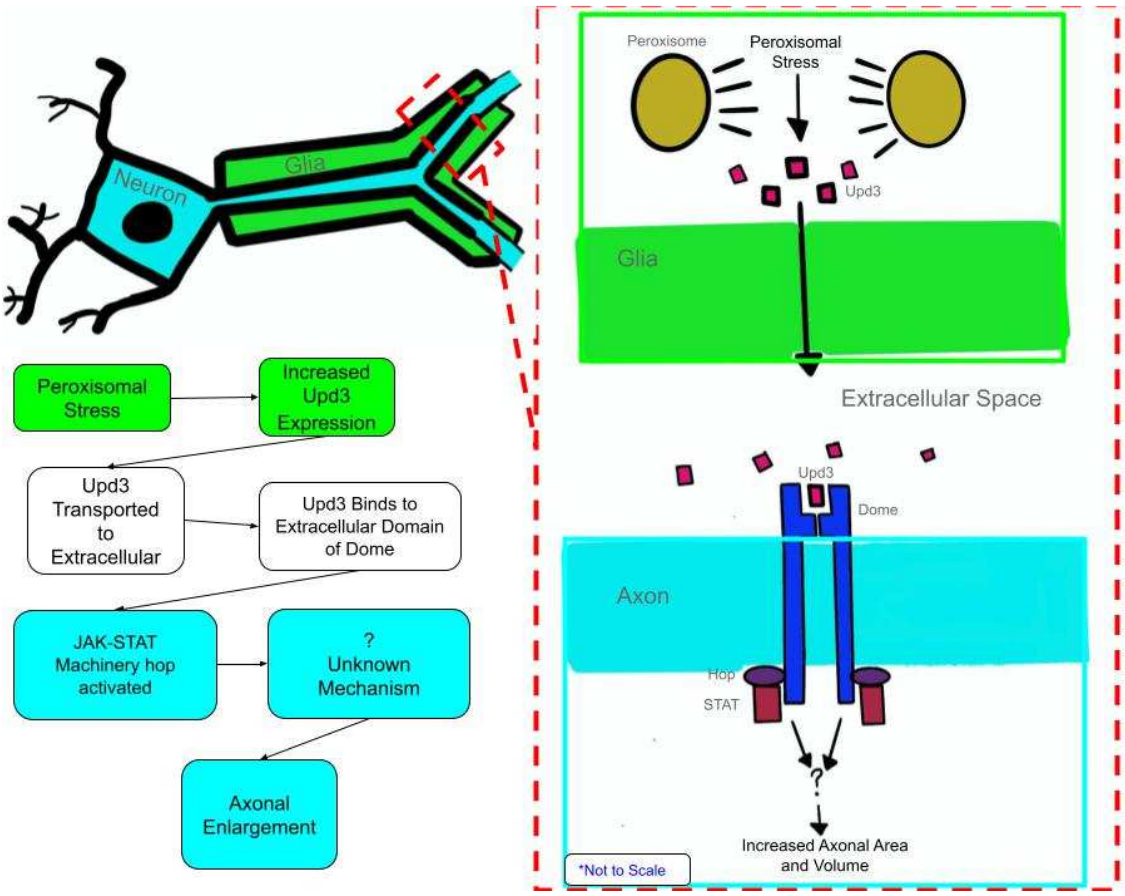

Figure 8: Model

Model based on results presented in this study. Peroxisomal stress, via RNAi knockdown of *Pex5*, signals for increase in cytokine upd3 within peripheral nervous system glia. Upd3 activates JAK-STAT pathway, including the hop component, which begins an inter-axonal mechanism leading to larger axon area and volume as well as motor ability deficit. Light Blue = Neuronal/Axonal Tissue. Green= Glial Tissue. White = Extracellular Space. Pink Squares = cytokine upd3. Dark Blue = dome receptor. Purple = hop. Magenta = STAT.

REFERENCES

Agaisse H., Perrimon N. (2004). The roles of JAK/STAT signaling in *Drosophila* immune responses. Immunological Reviews. *198*, 72-82.

Baumgart, E., Vanhorebeek, I., Grabenbauer, M., Borgers, M., Declercq, P.E., Fahimi, H.D., Baes, M. (2001). Mitochondrial Alterations Caused by Defective Peroxisomal Biogenesis in a Mouse Model for Zellweger Syndrome (*PEX5* Knockout Mice). Am. Journ. of Pathology. *159*, 1477-1494.

Birnbaum, A., Sodders, M., Bouska., Chang, K., Kang, P., McNeill, E., Bai, H. (2021). FOXO Regulates Neuromuscular Junction Homeostasis During *Drosophila* Aging. Front. Aging Neurosci. *12*.

Cara, F.D., Rachubinski, R.A., Simmonds, A.J. Distinct Roles for Peroxisomal Targeting Signal Receptors Pex5 and Pex7 in *Drosophila*. Genetics, *211(1)*, 141–149.

Chung, H. L., Wangler, M. F., Marcogliese, P. C., Jo, J., Ravenscroft, T. A., Zuo, Z., Duraine, L., Sadeghzadeh, S., Li-Kroeger, D., Schmidt, R. E., Pestronk, A., Rosenfeld, J. A., Burrage, L., Herndon, M. J., Chen, S., Members of Undiagnosed Diseases Network, Shillington, A., Vawter-Lee, M., Hopkin, R., Rodriguez-Smith, J., … Bellen, H. J. (2020). Loss- or Gain-of-Function Mutations in ACOX1 Cause Axonal Loss via Different Mechanisms. *Neuron*, *106*(4), 589–606.e6. https://doi.org/10.1016/j.neuron.2020.02.021

Copf, T., Goguel, V., Lampin-Saint-Amaux, A., Scaplehorn, N., & Preat, T. (2011). Cytokine signaling through the JAK/STAT pathway is required for long-term memory in *Drosophila.* Proceedings of the National Academy of Sciences of the United States of America. *108(1*9), 8059–8064. https://doi.org/10.1073/pnas.1012919108

Faust, J.E., Verma, A., Peng, C., McNew, J.A. (2012). An Inventory of Peroxisomal Proteins and Pathways in *Drosophila* melanogaster. Traffic. *13(10)*, 1378-1392.

Freeman M. R. (2015). *Drosophila* Central Nervous System Glia. *Cold Spring Harbor perspectives in biology*, *7*(11), a020552. https://doi.org/10.1101/cshperspect.a020552

Hartenstein, K. (2011). Morphological diversity and development of glia in *Drosophila*. Glia. *59(9)*, 1237-1252.

Hebbar, S., Hall, R.E., Demski, S.A., Subramanian, A., Fernandes J.J. (2006). The Adult Abdominal Neuromuscular Junction of *Drosophila*: A Model for Synaptic Plasticity. Journ. of Neurobiology. *66(10)*, 1140-1155.

Huang, K., Miao, T., Change, K., Kim, J., Kang, P., Jiang, Q., Simmonds, A.J., Cara F.D., Bai, H. (2020). Impaired peroxisomal import in *Drosophila* oenocytes causes cardiac dysfunction by inducing upd3 as a peroxikine. Nature Comm. *11*, 2943.

Jeibmann, A., & Paulus, W. (2009). *Drosophila* melanogaster as a model organism of brain diseases. International journal of molecular sciences, 10(2), 407–440. https://doi.org/10.3390/ijms10020407

Kassmann, C., Lappe-Siefke, C., Baes, M., Brügger, B., Mildner, A., Werner, B.H., Natt, O., Michaelis T., Prinz, M., Frahm J., and Nave, K. (2007). Axonal loss and neuroinflammation caused by peroxisome-deficient oligodendrocytes. Nature Genetics *39*, 969-976.

Lu, B., & Vogel, H. (2009). *Drosophila* models of neurodegenerative diseases. Annual review of pathology, 4, 315–342. https://doi.org/10.1146/annurev.pathol.3.121806.151529

Mackay, W.J., Bewley, G.C. (1989). The genetics of catalase in *Drosophila* melanogaster: isolation and characterization of acatalasemic mutants. Genetics. *122*, 643-652.

Myllymäki, H., Rämet, M. (2014). JAK/STAT Pathway in *Drosophila* Immunity. Scandinavian Journ. of Immunology. *76(6)*, 377-385.

Rasband, W. (2002). Voxel Counter. NIH.

Schindelin, J., Arganda-Carreras, I., Frise E., Kaynig, V., Longair, M., Pietzsch, T., Preibisch, S., Rueden, C., Saalfeld, S., Schmid, B., Tinevez, J.V., White, D.J., Hartenstein, V., Eliceiri, K., Tomancak, P., Cardona, A. (2012). Fiji: an open-source platform for biological-image analysis. Nature Methods. *9*, 676-682.

Stork, T., Engelen, A., Krudewig, A., Marion, S., Bainton, R.J., Klämbt, C. (2008). Organization and function of the Blood-Brain Barrier in *Drosophila*. J. Neurosci., *28(3)*, 587-597.

Wagner, N., Laugks, U., Heckmann, M., Asan, E., and Neuser, K. (2015). Aging *Drosophila* melanogaster display altered pre- and postsynaptic ultrastructure at adult neuromuscular junctions. J. Comp. Neurol. *523*, 2457–2475.

Wanders, R. J. & Waterham, H. R. (2006). Peroxisomal disorders: the single peroxisomal enzyme deficiencies. Biochim. Biophys. Acta. *1763*, 1707–1720.

Yan, Z., Gibson, S.A., Buckley, J.A., Qin, H., Benveniste, E.N. (2018). Role of the JAK/STAT signaling pathway in regulation of innate immunity in neuroinflammatory diseases. Clinical Immunology. *189*, 4-13.

Yeh, P.A., Liu, Y.H., Chu, W.C., Liu, J.Y., Sun, H.Y. (2018) Glial expression of disease-associated poly-glutamine proteins impairs the blood–brain barrier in *Drosophila*. Human Mol. Genetics. *27(14)*, 2546–2562.